



# Lawrence Berkeley Laboratory

UNIVERSITY OF CALIFORNIA

## CHEMICAL SCIENCES DIVISION

To be published as a chapter in *Gas Phase Chemical Reaction Systems: Experiments and Models: 100 Years After Max Bodenstein*,  
J. Wolfrum, H.-R. Volpp, R. Rannacher, and J. Warnatz, Eds. Springer-Verlag  
Berlin, Heidelberg, Germany, 1996

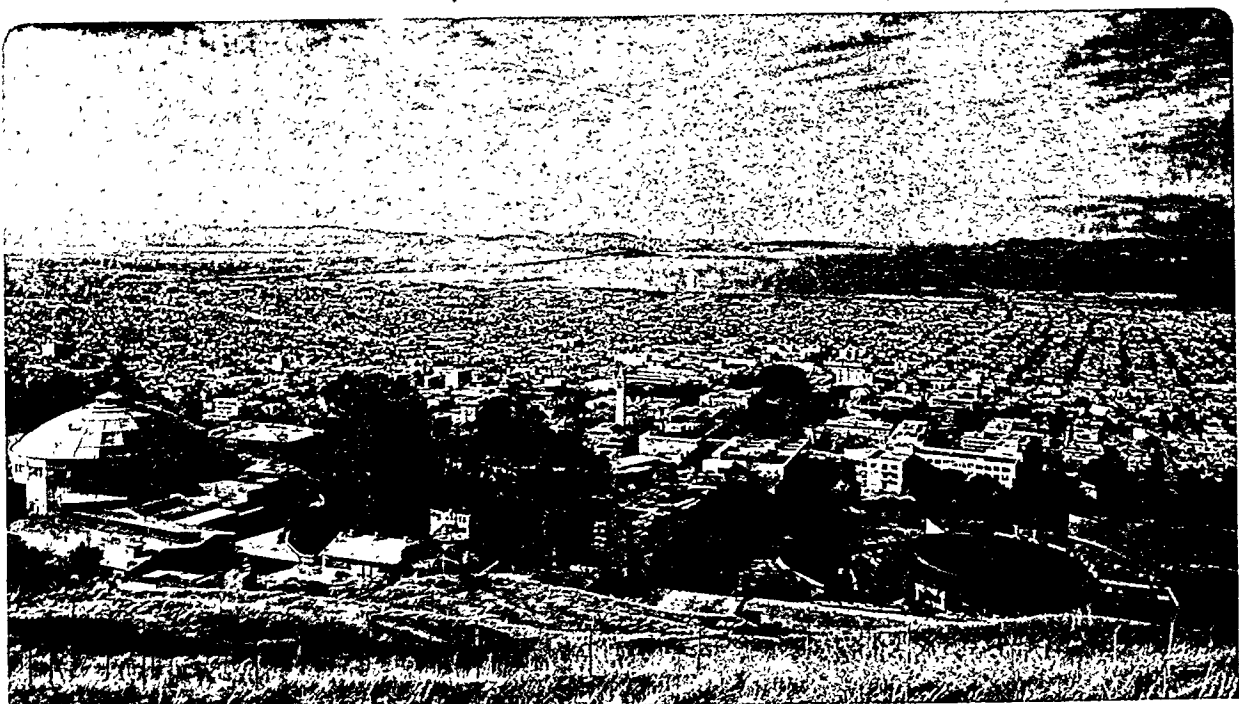
FEB 15 1996

OSTI

### The Reactions of Na<sub>2</sub> with O<sub>2</sub>

H. Hou, K.-T. Lu, V. Sadchenko, A.G. Suits, and Y.T. Lee

September 1995





#### DISCLAIMER

This document was prepared as an account of work sponsored by the United States Government. While this document is believed to contain correct information, neither the United States Government nor any agency thereof, nor The Regents of the University of California, nor any of their employees, makes any warranty, express or implied, or assumes any legal responsibility for the accuracy, completeness, or usefulness of any information, apparatus, product, or process disclosed, or represents that its use would not infringe privately owned rights. Reference herein to any specific commercial product, process, or service by its trade name, trademark, manufacturer, or otherwise, does not necessarily constitute or imply its endorsement, recommendation, or favoring by the United States Government or any agency thereof, or The Regents of the University of California. The views and opinions of authors expressed herein do not necessarily state or reflect those of the United States Government or any agency thereof, or The Regents of the University of California.

Ernest Orlando Lawrence Berkeley National Laboratory  
is an equal opportunity employer.



LBL-37699  
UC-401

## **The Reactions of Na<sub>2</sub> with O<sub>2</sub>**

Hongtao Hou, Kueih-Tzu Lu, Vladislav Sadchenko,  
Arthur G. Suits, and Yuan T. Lee

Department of Chemistry  
University of California, Berkeley

and

Chemical Sciences Division  
Lawrence Berkeley National Laboratory  
University of California  
Berkeley, California 94720

September 1995

This work was supported by the Director, Office of Energy Research, Office of Basic Energy Sciences,  
Chemical Sciences Division, of the U.S. Department of Energy under Contract No. DE-AC03-76SF00098.

DISTRIBUTION OF THIS DOCUMENT IS UNLIMITED ✓2

MASTER



# The Reactions of $\text{Na}_2$ with $\text{O}_2$

Hongtao Hou, Kueih-Tzu Lu[1], Vladislav Sadchenko[2], Arthur G. Suits and Yuan T. Lee[3]

*Department of Chemistry, University of California at Berkeley, and  
Chemical Sciences Division, Lawrence Berkeley National Laboratory  
Berkeley, CA 94720*

## I. Abstract

The reactions of  $\text{Na}_2$  with  $\text{O}_2$  were studied in a crossed-beam experiment at collision energies ( $E_c$ ) of 8 and 23 kcal/mol. The formation of  $\text{NaO}_2 + \text{Na}$  was observed at both collision energies, with the angular distributions of  $\text{NaO}_2$  in the center of mass coordinates peaking strongly forward with respect to the direction of the  $\text{O}_2$  beam, suggesting that the reaction is completed in a time scale that is shorter than one rotational period of the molecular system. From the velocity distribution of the products, we found that the newly formed  $\text{NaO}_2$  molecules are internally excited, with less than 20% of the available energy appearing in the translational motion of the separating products. These results indicate a “spectator stripping” mechanism for the reaction, with the  $\text{O}_2$  stripping one Na off the  $\text{Na}_2$  molecules. At  $E_c = 23$  kcal/mol the cross section for this reaction channel,  $\sigma_{\text{NaO}_2}$ , is estimated to be  $0.8 \text{ \AA}^2$ . Another reaction channel which produces  $\text{NaO} + \text{NaO}$  was seen at  $E_c = 23$  kcal/mol. The angular distribution for  $\text{NaO}$  is broad and forward-backward symmetric in the center of mass frame. A substantial fraction of the available energy is released into the relative motion of the products. This reaction is likely to proceed on an excited potential energy surface since a charge transfer to the excited  $\text{O}_2$  orbitals seems necessary for breaking the O-O bond. The measurement yields a bond energy of 60 kcal/mol for the  $\text{Na-O}$  molecule, and a total cross section of  $2 \text{ \AA}^2$  for this reaction channel at  $E_c = 23$  kcal/mol.

## II. Introduction

The reactions of alkali metals (M) with oxygen molecules have been studied for decades. In combustion processes, alkali atoms can rapidly form superoxides,  $\text{MO}_2$ , in an oxygen rich flame through recombination reactions such as  $\text{M} + \text{O}_2 + \text{N} \rightarrow \text{MO}_2 + \text{N}$  (where N is a third body).[4][5][6] The knowledge of the rate constants for these reactions and that for the unimolecular decomposition of  $\text{MO}_2$  is essential for modelling the kinetics of the combustion processes and calculating the composition of the free radicals in the flame. However, the alkali dimer reactions, which also produce  $\text{MO}_2$ , were often neglected in kinetics modelling because there was less information for these reactions. Although the concentration of the dimers in the flame is much lower than that of the monomers, it is still appreciable owing to the covalent bonding in the alkali dimer molecules, which is nearly 1 eV in strength. Further more, reactions of the dimers could be significant also because they produce  $\text{MO}_2$  via direct bimolecular reactions, which is expected to be faster than the three body recombinations between M and  $\text{O}_2$ . Therefore taking the dimer reactions into consideration could make substantial improvements over the existing kinetics models.

The various collisional processes of alkali atoms with oxygen molecules have been investigated extensively during the past fifteen years, especially the electronic excitations of the alkali atoms  $\text{M} + \text{O}_2 \rightarrow \text{M}^* + \text{O}_2$  at collision energies of  $2 \sim 10$  eV.[7] In the  $\text{Na} + \text{O}_2$  collision, Na D-line fluorescence was observed as the collision energy was increased above the  $3\text{P} \leftarrow 3\text{S}$  excitation energy of 2.1 eV, with its inten-

sity becoming stronger as the collision energy was increased. The cross section for this process was found to be  $26 \text{ \AA}^2$  at a collision energy of 5 eV. When the collision energy was above 8 eV, fluorescence from higher electronic states appeared. The inelastic scattering experiment of  $\text{Na}(4\text{D}) + \text{O}_2$  carried out in our lab[8] showed that the translational energy of the reactants could effectively promote Na to long-lived Rydberg states ( $\tau \geq 320 \mu\text{s}$ ). Kleyn and coworkers carried out landmark investigations of the charge transfer processes  $\text{M} + \text{O}_2 \rightarrow \text{M}^+ + \text{O}_2^-$  at collision energies ranging from 4 to 2000 eV.[9][10] In their experiment, the relative velocity of the reactants was so fast that the “collision time” was comparable with the vibrational period of the  $\text{O}_2^-$  ( $\omega_e = 1089 \text{ cm}^{-1}$ )[11]. Because the electron transfer probability and the critical distance vary strongly as a function of the internuclear distance of  $\text{O}_2^-$ , these authors observed oscillations in the differential cross sections. These results clearly demonstrated that the measurements of angular distributions of the scattered molecules could reveal not only the average lifetime of the collision complexes using the picosecond rotational period as an inherent clock, but also in the cases of charge transfer the vibrational motions of the reaction intermediates on the time scale of  $\sim 100$  femtoseconds. In all these processes mentioned above, charge transfer from alkali metal to  $\text{O}_2$  molecules was undoubtedly the essential first step to account for the change of the electronic states of the alkali atoms in these experiments; and the behavior of the ionic intermediate  $\text{M}^+\text{O}_2^-$  determines the outcomes of the scattering. The chemical reaction  $\text{M} + \text{O}_2 \rightarrow \text{MO} + \text{O}$  however, was not seen in the previous studies.

Alkali dimers have many interesting properties[11][12][13] that make their chemistry very unique. The ionization potentials of the dimer molecules are lower than those of the corresponding monomers such that when dimers interact with electron accepting molecules, the ionic and covalent potential energy surfaces cross at larger intermolecular distances, which could strongly affect the charge transfer probabilities and the overall reaction cross sections. The bond lengths of  $\text{M}_2$  and  $\text{M}_2^+$  are extraordinarily long (e. g. 3.0  $\text{\AA}$  for  $\text{Na}_2$ , 3.5  $\text{\AA}$  for  $\text{Na}_2^+$ ) and although the bond length of  $\text{M}_2^+$  is longer, the bond dissociation energy of  $\text{M}_2^+$  ion is  $\sim 50\%$  higher than those of  $\text{M}_2$  neutrals. The covalent bonds of the alkali dimers are abnormally weak, with the bond dissociation energies lower than 1 eV, making many chemical reactions involving the cleavage of the alkali dimer bonds exoergic.

Figger and coworkers[14] observed chemiluminescence in their crossed-beam experiment of alkali metal dimers with oxygen molecules. In the reactions of  $\text{Cs}_2$ ,  $\text{Rb}_2$ ,  $\text{K}_2$  and  $\text{Li}_2$ , D-line emissions as well as continuous chemiluminescence from the collision zone were recorded. They attributed them to the formation of electronically excited products from the reactions  $\text{M}_2 + \text{O}_2 \rightarrow \text{MO}_2 + \text{M}^*$  and  $\text{M}_2 + \text{O}_2 \rightarrow \text{MO}_2^* + \text{M}$ . No emission was observed for the  $\text{Na}_2$  reactions due to their lower exothermicities.

Very recently, Goerke and coworkers[15] reported the results of their studies on the reactions of sodium clusters with oxygen molecules using photoionization and ion time-of-flight as detection methods.  $\text{Na}_n\text{O}$  ( $2 \leq n \leq 4$ ) and  $\text{Na}_m\text{O}_2$  ( $2 \leq m \leq 6$ ) products were detected for the reactions of  $\text{Na}_x$  ( $3 \leq x \leq 8$ ) with  $\text{O}_2$ . Angular distributions of  $\text{Na}_n\text{O}$  ( $2 \leq n \leq 4$ ) and  $\text{Na}_m\text{O}_2$  ( $2, 3, 5$ ) showed strong forward scattering with respect to the sodium cluster beam in the center of mass frame. Although the energy distributions of the products were not measured, their experimental data suggested that most of the exothermicity remained in the internal degrees of freedom of the products. The cross sections for the reactions were determined to be  $50 \sim 80 \text{ \AA}^2$ , which led to their conclusion that electron harpooning[16][17][18][19] was the first step in the course of the reactions. However, these authors didn't include  $\text{Na}_2$  reactions into their consideration. Meanwhile, due to the high ionization potential of  $\text{NaO}$  and  $\text{NaO}_2$  they were not able to detect these molecules with the photon energy used in their experiments, although the presence of these molecules was almost certain.

This paper presents our results from crossed-beam studies of the reactions of sodium dimers with oxygen molecules. For this seemingly simple chemical system, there are at least four distinct reaction pathways that were energetically accessible under our experimental conditions:



The energetics for these reactions[11][12][13] are plotted in Fig. 1. Reaction (i) is the only exothermic reaction and it becomes Reaction (iv) in the case when the internal excitation of  $\text{NaO}_2$  along the  $\text{Na}-\text{O}_2$  bond exceeds its dissociation limit. In our experiment, we measured the angular and velocity distributions of the products at two collision energies, which enabled us to identify the important reaction channels and learn the dynamics underlying these molecule-molecule collision processes.

### III. Experimental

The details of the crossed-beam apparatus used in our experiment can be found in many earlier publications.[20][21] Briefly, the alkali dimer source consisted of a resistively heated molybdenum oven and nozzle assembly, with the temperatures of the nozzle and the oven being controlled independently by different heating elements. Sodium vapor carried by an inert gas, which was either He or Ne, expanded out of the 0.2 mm diameter nozzle to form a supersonic beam of  $\text{Na}/\text{Na}_2/\text{inert gas}$  mixture.  $\text{Na}_2$  concentration was about 5% molar fraction of the total sodium in the beam when He was used as carrier gas. The beam quality dropped severely when we seeded  $\text{Na}_2$  in Ne so the dimer intensity became much weaker. No substantial amount of trimers or larger clusters was detected under our experimental conditions.  $\text{Na}_2$  beam was crossed at  $90^\circ$  by a neat oxygen supersonic beam in the main collision chamber under single collision conditions. The  $\text{O}_2$  source nozzle was heated to  $473^\circ\text{K}$  to prevent cluster formation. Both sources were doubly differentially pumped. The beams were skimmed and collimated to  $2^\circ$  FWHM in the collision chamber. Under these conditions, the collision energies for the reaction could be varied from 8 kcal/mol to 23 kcal/mol.

A rotatable detector combining a quadrupole mass spectrometer and a Daly type ion counter was used to measure the angular and velocity distributions of the products in the molecular beam-defined plane. A fraction of the neutral products entering the detector were ionized by 200 eV electron bombardment. Ions formed in the ionization region were extracted into a quadrupole mass filter which was set to have unit mass resolution. The products were modulated at the entrance of the detector with a double-sequence pseudorandom mechanical chopping wheel.[21] The number density of a certain mass was recorded as a function of the flight time that the molecules spent to travel through the distance from the chopping wheel to the ion counter. Neutral time-of-flight spectra were obtained by deconvolving the recorded signal over the chopper gating function and subtracting the ion flight time from ionizer to the ion counter. Under our experimental conditions, we were unable to measure the signal close to the  $\text{Na}_2$  beam. At these angles, the number density of elastically scattered Na was very high such that a certain fraction of scattered Na could be excited to long-lived Rydberg states by electron bombardment and subsequently field-ionized in the ion counting region. The mass spectrometer was “transparent” to these Rydberg atoms so they became strong interference at all the masses of interest. We also

recorded the spectra for O and O<sub>2</sub> but the effort to extract any information related to reactions was not successful because of the high background of oxygen in the mass spectrometer and the intense nonreactive scattering of the O<sub>2</sub>.

#### IV. Results and kinematic analysis

In our experiment, we observed NaO<sup>+</sup> (m/e = 39) signal which was unambiguously from the reactive scattering since it contains both Na and O. The monomer reaction Na + O<sub>2</sub> → NaO + O has very large endothermicity ( $\Delta D_0 = + 58$  kcal/mol[12]). Under our experimental conditions, even the highest collision energy for Na + O<sub>2</sub> was not sufficient for this reaction to happen. Thus the observed NaO<sup>+</sup> signal must be from the reactions of sodium dimers with oxygen molecules. This result is in contradiction with that reported by Goerke et al.[15] who explicitly ruled out the possibility of the dimer reactions in their similar experiment. Neither NaO<sub>2</sub><sup>+</sup> nor Na<sub>2</sub>O<sup>+</sup> signal was seen under our experimental conditions. However this does not necessarily mean that only Reaction (iii) took place. In the ionization region, electron impact fragmentation is severe, especially for the internally excited molecules. Both NaO<sub>2</sub> from Reaction (i) and Na<sub>2</sub>O from Reaction (ii) could fragment completely and both molecules could form NaO<sup>+</sup>. Additional analysis on the kinematics and dynamics of the reactions have to be made in order to identify the actual reaction pathway(s).

##### A. Collision Energy at 8 kcal/mol

The Newton diagram[22][23][24] for Na<sub>2</sub> + O<sub>2</sub> at a nominal collision energy of 8 kcal/mol is shown in Fig. 2.  $\Theta_{CM}$  denotes the laboratory angle of the center of mass velocity vector for Na<sub>2</sub> + O<sub>2</sub>. For future discussions, we also plotted the center of mass velocity (dotted line) for Na + O<sub>2</sub>, which extends an angle of  $\Theta_m$  from the Na<sub>2</sub> beam. The direction of the Na<sub>2</sub> velocity in the center of mass frame is defined as 0° hereafter. At this collision energy, only Reaction (i) could take place, so the observed NaO<sup>+</sup> signal was entirely due to the fragmentation of NaO<sub>2</sub> products. The solid circle in Fig. 2 encloses the zone within which NaO<sub>2</sub> might appear. Fig. 3 shows the NaO<sup>+</sup> time-of-flight spectra recorded at several laboratory angles. Beyond the range of these angles, the signal became too weak to observe the time-of-flight peaks. It was observed that most NaO<sub>2</sub> products appeared around  $\Theta_m$ . Signal intensities obtained by integrating the time-of-flight spectra are plotted in Fig. 4 to give the laboratory angular distribution for NaO<sub>2</sub>. Compared with the range that the NaO<sub>2</sub> circle extends to in the Newton diagram, the NaO<sub>2</sub> angular distribution was very narrow.

In Fig. 3 and Fig. 4, the solid lines are the computer simulation of the data obtained by assuming certain center of mass translational energy distribution (P(E)) and angular distribution (T( $\Theta$ )) shown in Fig. 5. Peaking at the direction of the O<sub>2</sub> beam (180°), the angular distribution shows remarkable anisotropy, with all the NaO<sub>2</sub> products scattered into the hemisphere towards the O<sub>2</sub> beam. This anisotropy indicates that the reaction takes place during a time that is shorter than the rotational period of the molecular system so that the products are separated before they lose the information of the well defined approaching direction of the reactants.[24] At this collision energy, the total available energy for the reaction (E<sub>c</sub> +  $\Delta D_0$ ) is 34 kcal/mol, among which only an average of 2.6 kcal/mol appears in the translational motion of the products (cf. P(E) in Fig. 5). The rest of the energy has to become the internal excitation of the NaO<sub>2</sub> molecules. When NaO<sub>2</sub> is ionized to form NaO<sub>2</sub><sup>+</sup>, the binding energy between Na<sup>+</sup> and O<sub>2</sub> becomes weaker and the internal excitation initially stored in NaO<sub>2</sub> is likely to remain in NaO<sub>2</sub><sup>+</sup> and causes the complete dissociation of NaO<sub>2</sub><sup>+</sup> into Na<sup>+</sup> and O<sub>2</sub>. This is probably the reason why NaO<sub>2</sub><sup>+</sup> parent ion was not detected. However when NaO<sub>2</sub> is excited to higher electronic states during the electron impact ionization, the dissociative ionization could produce a stable NaO<sup>+</sup> ion.

### B. Collision Energy at 23 kcal/mol

All the dimer reactions (i) ~ (iv) became energetically accessible at a collision energy of 23 kcal/mol. The Newton diagram for this collision energy is shown in Fig. 6. For Reaction (ii), the available energy was only 5 kcal/mol. The heavier products  $\text{Na}_2\text{O}$  (compared with  $\text{O}$ ) have to be limited in the small circle. On the other hand,  $\text{NaO}$  molecules produced by Reaction (iii) are much less confined because there was slightly more available energy (9 kcal/mol) and no disparity in the masses of the products. The time-of-flight spectra of  $\text{NaO}^+$  recorded at different laboratory angles are plotted in Fig. 7, and the laboratory angular distribution of the  $\text{NaO}^+$  intensity is shown in Fig. 8. There are clearly two features in the time-of-flight spectra. Both features exist well out of the  $\text{Na}_2\text{O}$  limit which indicates clearly that the observed signal was not from Reaction (ii). The slow peaks which appear at  $\sim 120 \mu\text{s}$  have a very narrow angular distribution, with the intensity peaking sharply around  $\Theta_m$ . The angular and velocity distributions of this slow signal bear such strong resemblances to those of the  $\text{NaO}_2$  products we saw at low collision energy that it is with little doubt to assign this signal to the same reaction channel. The fast peaks, arriving at  $\sim 70 \mu\text{s}$ , have very different characteristics than those of the  $\text{NaO}_2$  products. Appearing weak at all angles and becoming only slightly stronger at small angles, these fast peaks have much less variation in the intensity, an indication of products with larger recoil velocities and broader laboratory angular distributions. Therefore this fast signal is, without any doubt, the  $\text{NaO}$  products from Reaction (iii).

The simulation of the time-of-flight and angular distribution data was done by assuming an independent set of  $P(E)$  and  $T(\theta)$  for each reaction channel. An additional parameter  $\gamma$  was assigned to each reaction channel to weight its contribution to the observed signal. The total fits are plotted in solid lines in Fig. 7 and Fig. 8. The dotted lines and the dashed lines show the contributions from Reaction (i) and Reaction (iii), respectively. Fig. 9 shows the  $P(E)$  and  $T(\theta)$  for Reaction (i). As mentioned above, these distributions are similar to those at low collision energy.  $T(\theta)$  again peaks sharply at the direction of  $\text{O}_2$  beam with all the  $\text{NaO}_2$  scattered into the  $\text{O}_2$  hemisphere, showing strong anisotropy. Among the 49 kcal/mol available energy, only an average of  $\sim 8$  kcal/mol was released into the translational energy of the separating products. The  $P(E)$  has a sharp rising edge at  $\sim 7$  kcal/mol, which indicates that the internal energy of  $\text{NaO}_2$  could not exceed 42 kcal/mol or else the  $\text{NaO}_2$  molecule could not be held together. The subsequent result is the collisional dissociation making  $\text{Na} + \text{Na} + \text{O}_2$ . Therefore this sharp rising edge in  $P(E)$  marks the onset of Reaction (iv), which requires at least the energy to break the Na-Na bond. The collision energy of 23 kcal/mol less the cut off energy of 7 kcal/mol in the  $P(E)$  is then our experimental measurement of the Na-Na bond dissociation energy. The result of 16 kcal/mol is in agreement with the well known value in the literature.[12]

Fig. 10 shows the  $P(E)$  and  $T(\theta)$  used in the simulation of Reaction (iii). The angular distribution is quite broad. The forward-backward symmetry in the product angular distribution is a prerequisite rather than an experimental result because in this reaction two identical molecules are always produced with exactly opposite center of mass velocities. Under such conditions the angular distribution does not tell us the time duration of the reaction, which is the important information for dynamics studies. The  $P(E)$  shows that an average of 3 kcal/mol is released in the translational motion of the products. The high energy cut off at 5.5 kcal/mol in the  $P(E)$  allows us to estimate Na-O bond strength. From the conservation of energy, there is the following relation between the energies of the reactants and the products:

$$E'_{\text{trans}} + E'_{\text{int}} = E_{\text{trans}} + E_{\text{int}} + \Delta D_0 \quad (1)$$

where  $E_{\text{trans}}$  and  $E'_{\text{trans}}$  are the center of mass translational energies of the reactants and products, respectively. Similarly,  $E_{\text{int}}$  and  $E'_{\text{int}}$  are the internal energies, i.e. the total electronic, vibrational and rotational energies, in the reactants and the products, respectively.  $\Delta D_0$  is the change of the bond dissociation energy for the reaction.  $E_{\text{int}}$  is assumed to be negligible for the supersonic beams.  $E'_{\text{trans}}$  reaches its maximum value when  $E'_{\text{int}}$  is the minimum, which will be assumed to be zero, namely at the highest translational energy release, both NaO products are assumed to be in the ground state. From Equation (1) and the maximum translational energy release in the P(E), we calculated the change of bond dissociation energy  $\Delta D_0$  for Reaction (iii) to be -17 kcal/mol. Using the accurately known values of  $D_0(\text{O-O})$ , 119 kcal/mol, and  $D_0(\text{Na-Na})$ , 18 kcal/mol,[12] we obtained  $D_0(\text{Na-O}) = 60$  kcal/mol, which can be compared with the literature value of  $61.2 \pm 4.0$  kcal/mol.[12]

From the best fit, the relative contributions of these two reactions to the observed signal at  $m/e = 39$  are:

$$\gamma_i : \gamma_{\text{iii}} = 1 : 1.8. \quad (2)$$

In Equation (2), we use the subscripts to denote the reaction channels.

In order to estimate the cross sections for the reactions, we also measured the time of flight spectra for the  $\text{Na}^+$  signal under the same experimental conditions. It is known that both NaO and  $\text{NaO}_2$  dissociate heavily to  $\text{Na}^+$  under electron impact.[25][26] The collisional dissociation Reaction (iv), if present, would also generate  $\text{Na}^+$ . But most  $\text{Na}^+$  detected came from elastic/inelastic scattering of the Na monomer with  $\text{O}_2$  because the number density of the monomers at the collision zone was roughly 20 times higher than that of the dimers.  $\text{Na}^+$  time-of-flight spectra at  $25^\circ$  and  $30^\circ$  are given in Fig. 11. At these angles, the nonreactive scattering of  $\text{Na}_2$  was negligible. For comparison, the scattering signal of Na from  $\text{N}_2$  at corresponding angles was also measured and is plotted in the same figure. The differences due to the reactions are obvious. We can fit the  $\text{Na}^+$  spectra for  $\text{Na}/\text{Na}_2 + \text{O}_2$  scattering with four different channels: the elastic scattering from  $\text{Na} + \text{O}_2$ , the inelastic scattering from  $\text{Na} + \text{O}_2$ , Reaction (i) from  $\text{Na}_2 + \text{O}_2$  and Reaction (iii) from  $\text{Na}_2 + \text{O}_2$ . We use the same translational energy and angular distributions as those for the  $\text{NaO}^+$  signals to fit the reactive signals in the  $\text{Na}^+$  spectra although we have to use different weights ( $\gamma'$ ) to account for the different fragmentation patterns of NaO and  $\text{NaO}_2$  in the ionization region. The results are also plotted in Fig. 11, where the solid lines show the overall fit and the broken lines indicate the contribution from each individual channels, as described in detail in the figure captions. The discrepancies between the fit and the data are possibly due to the collisional dissociation Reaction (iv), which is difficult to account for because it is a three body event. Nevertheless, leaving Reaction (iv) out will not affect our final results of obtaining the cross sections for Reaction (i) and Reaction (iii) because we are comparing these reaction channels with the nonreactive signal only. From the fit, the relative weight for each channel is:

$$\gamma'_{\text{elastic}} : \gamma'_{\text{inelastic}} : \gamma'_i : \gamma'_{\text{iii}} = 105 : 171 : 0.5 : 3.0. \quad (3)$$

Because we did not observe any  $\text{NaO}_2$  signal, it is safe to assume that  $\text{NaO}_2$  molecules, if ionized, dissociated completely to either  $\text{NaO}^+$  or  $\text{Na}^+$ . Fig. 12 illustrates the relations between the parent molecules directly from the scattering and the measured signal, which will serve as a road map for our discussions in the following sections. Here  $\sigma_i$  and  $\sigma_{\text{iii}}$  are the reaction cross sections for Reaction (i) and Reaction (iii), respectively.  $\sigma_{\text{elastic}}$  and  $\sigma_{\text{inelastic}}$  are the cross sections for the elastic scattering and

the inelastic scattering of  $\text{Na} + \text{O}_2$ .  $\sigma_{\text{ion}}(X)$  denotes the ionization cross section of molecule X by electron bombardment. The ions so formed undergo further dissociation to give the observed signal. We define  $\xi$  as the fraction of  $\text{NaO}^+$  among the total Na-containing positive ions produced by electron bombardment. According to the assumption that  $\text{NaO}_2$  dissociate completely upon electron bombardment, the fraction of  $\text{Na}^+$  from  $\text{NaO}_2$  is  $(1-\xi)$ . In a similar way, we define the fraction of  $\text{Na}^+$  among the total Na-containing positive ions produced from ionization of  $\text{NaO}$  products to be  $\eta$ . Accordingly the branching ratio between Reaction (i) and Reaction (iii) can be obtained. From Equation (2), we have:

$$\gamma_i : \gamma_{\text{iii}} = [\sigma_{\text{ion}}(\text{NaO}_2) \times \sigma_i \times \xi] : [2 \times \sigma_{\text{ion}}(\text{NaO}) \times \sigma_{\text{iii}} \times (1-\eta)] = 1 : 1.8. \quad (4)$$

The factor "2" accounts for the fact that two  $\text{NaO}$  were produced in Reaction (iii). Similarly, from Equation (3), we draw another relation between  $\sigma_i$  and  $\sigma_{\text{iii}}$ :

$$\gamma'_i : \gamma'_{\text{iii}} = [\sigma_{\text{ion}}(\text{NaO}_2) \times \sigma_i \times (1-\xi)] : [2 \times \sigma_{\text{ion}}(\text{NaO}) \times \sigma_{\text{iii}} \times \eta] = 0.5 : 3.0. \quad (5)$$

In order to compare the cross section for each channel, we need the knowledge of the ionization cross sections for Na,  $\text{NaO}$  and  $\text{NaO}_2$  by 200 eV electron bombardment. The ionization cross section of Na is known[27],  $\sigma_{\text{ion}}(\text{Na}) = 2.46 \text{ \AA}^2$ . The ionization cross section of  $\text{NaO}$  can be estimated[28] from the ionization cross section of  $\text{O}_2$ , and the ratio of the polarizabilities( $\alpha$ 's) of  $\text{O}_2$ [12] and  $\text{NaO}$  using the following equation:

$$\sigma_{\text{ion}}(\text{O}_2) : \sigma_{\text{ion}}(\text{NaO}) = \alpha_{\text{O}_2} : \alpha_{\text{NaO}} = 1.58 : 3.05, \quad (6)$$

where  $\alpha_{\text{NaO}}$  was obtained by adding the polarizability of  $\text{Na}^+$ ,  $\alpha_{\text{Na}^+} = 0.155 \text{ \AA}^3$ , and the polarizability of  $\text{O}^-$ ,  $\alpha_{\text{O}^-} = 2.85 \text{ \AA}^3$ . The result is  $\sigma_{\text{ion}}(\text{NaO}) = 5.2 \text{ \AA}^2$ . Similarly, we can calculate the ionization cross section for  $\text{NaO}_2$ , which gives  $\sigma_{\text{ion}}(\text{NaO}_2) = 6.5 \text{ \AA}^2$ .

Covinsky[25] measured  $\eta$  as a function of internal excitation of  $\text{NaO}$  in the  $\text{Na} + \text{O}_3$  experiment.  $\eta$  is roughly 0.8 for internally cold  $\text{NaO}$  (which was the case in this experiment because there is very little excess energy for Reaction (iii) and a considerable amount of this excess energy was released into the translational motion of the products). Using this value, we obtained  $\xi = 0.45$  and  $\sigma_i : \sigma_{\text{iii}} = 1 : 2.5$ .

The next step is to compare the reactive signal with the total nonreactive scattering. From Equation (3), we have the following relations:

$$\frac{\gamma'_i}{\gamma'_{\text{elastic}} + \gamma'_{\text{inelastic}}} = \frac{\sigma_{\text{ion}}(\text{NaO}_2) \times \sigma_i \times (1-\xi)}{20 \times \sigma_{\text{ion}}(\text{Na}) \times \sigma_{\text{Nonreactive}}} = \frac{0.5}{276}, \quad (7)$$

and

$$\frac{\gamma'_{\text{iii}}}{\gamma'_{\text{elastic}} + \gamma'_{\text{inelastic}}} = \frac{2 \times \sigma_{\text{ion}}(\text{NaO}) \times \sigma_{\text{iii}} \times \eta}{20 \times \sigma_{\text{ion}}(\text{Na}) \times \sigma_{\text{Nonreactive}}} = \frac{3.0}{276}, \quad (8)$$

where  $\sigma_{\text{Nonreactive}}$  is the sum of the cross sections of elastic scattering and inelastic scattering of  $\text{Na} + \text{O}_2$ . We added factors "20" in Equation (7) and Equation (8) because the number density of the monomers in the collision zone was roughly 20

times higher than that of the dimers. The interaction between Na monomer and O<sub>2</sub> becomes strong at the crossing of the covalent and ionic surfaces because of the charge transfer. If we neglect the long range van der Waals interaction, the internuclear distance at the surface crossing could be estimated using the following equation which is based on simple “Harpoon Mechanism”:[16][17][18][19]

$$R_c = \frac{14.4}{IP_{Na}(\text{eV}) - EA_{O_2}(\text{eV})} \quad (\text{\AA}), \quad (9)$$

where IP is the ionization potential of Na[12] and EA is the electron affinity of O<sub>2</sub>[12], both in the units of electron volts. Equation (9) gives a value of 3.1 Å for R<sub>c</sub>, which is larger than the averaged hard sphere radius between Na and O<sub>2</sub>. Since there is no reaction between Na monomer and O<sub>2</sub>, we can assume R<sub>c</sub> to be the nonreactive collision radius. Therefore we obtained the total nonreactive scattering cross section to be:  $\sigma_{\text{Nonreactive}} = \pi R_c^2 = 30 \text{ \AA}^2$ . Using these numbers in Equation (7) and Equation (8), we obtained the cross sections for Reaction (i),  $\sigma_i = 0.8 \text{ \AA}^2$  and Reaction (iii),  $\sigma_{\text{iii}} = 2 \text{ \AA}^2$ .

## V. Discussion

The MO<sub>2</sub> molecules have been studied quite extensively in the past. Alexander generated semiempirical potential energy surfaces for LiO<sub>2</sub> and NaO<sub>2</sub>.[29] He showed that the ground state NaO<sub>2</sub>, which was 1.6 eV more stable than the separated ground state Na and O<sub>2</sub>, had C<sub>2v</sub> geometry with Na at the apex of an isosceles triangle. The interaction within the molecule could be best described as Na<sup>+</sup>...O<sub>2</sub><sup>-</sup> singly charged ionic bonding. This is in accord with the Infrared and Raman[30][31] or ESR[32] spectroscopy results in low temperature matrices. Calculations on the NaO molecule also indicates that it is singly ionic, Na<sup>+</sup>...O<sup>-</sup>.[33] These results suggest that during the course of Reaction (i) and Reaction (iii), the Na<sub>2</sub> + O<sub>2</sub> system has to experience a change from covalent character to ionic nature. This resembles the well known M/M<sub>2</sub> + Halogen molecules (XY) reactions and was commonly characterized by the Harpoon Mechanism. Nevertheless, the Na<sub>2</sub> + O<sub>2</sub> reaction shows very different results than the M/M<sub>2</sub> + XY system. In the case of M<sub>2</sub> + XY,[34] for example, the main pathways have both M<sub>2</sub> and XY dissociate to form MX + M + Y or MX + MY with the total cross sections larger than 100 Å<sup>2</sup>. For the MX + M + Y channel, the MX product peaked strongly toward the M<sub>2</sub> direction in the center of mass velocity space.

M<sub>2</sub> + XY reactions are model systems that proceed via a long range electron transfer mechanism. Due to the low ionization potential of M<sub>2</sub> and high electron affinity of XY, the potential energy surfaces of the ionic state (M<sub>2</sub><sup>+</sup>...XY) and the covalent state (M<sub>2</sub>...XY) intersect at intermolecular distance R<sub>c</sub> = 7-8 Å (Equation (9)) which is much larger than the “hard sphere” radius. At this internuclear distance, there is a fair chance for the valence electron to “jump” from M<sub>2</sub> to the XY. A vertical ionization from the outer turning point of ground state M<sub>2</sub> puts M<sub>2</sub><sup>+</sup> in the attractive well and vertical ionization from the inner turning point sets M<sub>2</sub><sup>+</sup> on slightly repulsive (1 eV/Å) surface. Because the M<sub>2</sub><sup>+</sup> is almost 50% more strongly bound than M<sub>2</sub>,[13] along with the fact that both M<sub>2</sub> and M<sub>2</sub><sup>+</sup> have very low vibrational frequencies, the two alkali nuclei will separate only very slowly after electron transfer. On the other hand the XY<sup>-</sup> bonding is much weaker than that of XY neutral molecule. Vertical Frank-condon transition puts XY<sup>-</sup> on a very strong repulsive wall (6 eV/Å) above its dissociation limit primarily due to the strong antibonding orbital σ<sub>pz</sub>\*. As a result, X<sup>-</sup> and Y separate promptly after the vertical electron transfer while the M and M<sup>+</sup> will linger together for longer time. The reaction proceeds as if the M<sub>2</sub><sup>+</sup> “strips” the X<sup>-</sup> off to form the M<sub>2</sub>X molecules which peak preferentially towards the M<sub>2</sub> direction, leav-

ing the other halogen atom Y as a “spectator”. The highly vibrationally excited  $M_2X$  nascent molecule then boils off an M atom to form the final MX product. The initial repulsive force between the two halogens is offset by their attraction at longer distance as the two halogen atoms separate. consequently, the spectator Y does not carry away much of the excess energy.

For the  $Na_2 + O_2$  system, the scenario is quite different.  $O_2$  has a much lower electron affinity of 0.44 eV[12] so that the nominal crossing distance  $R_c$  calculated from Equation (9) is only 3.2 Å and only collisions with impact parameter smaller than  $R_c$  will experience the electron transfer. This limits the total cross section for charge transfer to be  $32 \text{ \AA}^2$  at most. Nevertheless, at such short intermolecular distance, the interaction between the ionic surface and the covalent surface is very strong. Once the system arrives at this region, it will have an almost unit probability to switch from covalent surface to ionic surface adiabatically. The final outcome of the reaction is determined by the interaction between  $Na_2^+$  and  $O_2^-$  after the electron transfer. Unlike the case of XY, the  $O_2^-$  bond is only slightly longer than that of  $O_2$  and the binding energy is almost as large. Vertical transition from  $O_2$  to the ground state of  $O_2^-$  would put  $O_2^-$  in the deep potential well. It takes some extra 90 kcal/mol in order to break  $O_2^-$  to form  $O + O^-$ . On the other hand, the weakly bound  $Na_2^+$  is much more vulnerable to dissociate into  $Na + Na^+$  under the influence of the strong Coulomb attraction. In the case when the impact parameter is large, there is little chance to cleave the  $O_2^-$  molecule during the time when two molecules glance off each other. Strong Coulomb interaction between  $Na^+$  and  $O_2^-$  leads to the formation of  $NaO_2$  molecules that are highly excited along the newly formed bonds. The departing Na atom should hardly be affected during the collision because the interaction between  $Na^+$  and Na is relatively weak compared with the Coulomb interaction between  $Na^+$  and  $O_2^-$ . Therefore it acts similarly as the “spectator” in the cases of the halogen reactions. The most important role for this Na atom is to carry away the excess energy partly through the breaking of the na-Na bond, much like a “third body” as in the recombination reactions, which is the reason why the  $NaO_2$  products are most likely to appear at  $\Theta_m$  — the result is just like a simple recombination of Na and  $O_2$ . Using this “spectator stripping” model, we can calculate the translational energy releases for  $E_c = 8$  and 23 kcal/mol to be 2.4 and 6.6 kcal/mol, respectively, matching well with the peaks in the corresponding P(E)’s.

It is worth pointing out that the formation of  $NaO_2$  results from the transfer of only one electron from  $Na_2$  to  $O_2$ . If both valence electrons are transferred to  $O_2$ , the molecular system is likely to sample the deep well on the potential energy surface, forming  $Na_2O_2$  complex (cf. Fig. 1). Since  $Na_2O_2$  complex dissociates mainly through the low energy channel, forming  $NaO_2 + Na$ , we would expect to see for the  $NaO_2$  products a forward-backward symmetric angular distribution, which is a characteristic for the complex formation. However in the experiments we observed a very anisotropic angular distribution. Therefore the complex formation mechanism can be excluded.

Contrary to the spectator mechanism of Reaction (i), Reaction (iii) requires considerable rearrangement of the electronic configuration of the system. First of all, both valence electrons have to be transferred because each  $NaO$  molecule has  $Na^+...O^-$  singly ionic character. This requires a close collision and a favorable approaching geometry between the reactants. This was not directly observed for this reaction because the symmetric angular distribution determined by the kinematics does not provide us much information of the scattering. But evidence could be found from the chemi-ionization reaction  $Ba + Cl_2 \rightarrow BaCl^+ + Cl^-$  in which case  $BaCl^+$  is backward scattered with respect to the Ba beam, demonstrating that the favored geometry for transferring two electrons is a collinear head-on collision.[36] Second, the strong O-O bond has to be broken. The exact pathways leading to the breaking of the O-O bond could not be deduced from our data, but some insights could be gained

by looking at the early results of dissociative attachment of  $O_2$ , and the results of our recent *Ab initio* calculations[37] using *Gaussian 92*. The formation of  $O + O^-$  by electron attachment was studied in great detail and a single electronically excited state  $^2\Pi_u$  was found to be responsible for this process, although there are many other states in the vicinity. The state specificity is largely due to the symmetry restriction which could be removed in the case of chemical reaction with the presence of the Na atoms. But the results do suggest that the breaking of the O-O bond is likely initiated by an electron transfer to the excited  $O_2^-$  orbital, which will result in a substantial bond stretching in  $O_2^-$ . The argument that the excited  $O_2^-$  orbital is important to the  $NaO + NaO$  reaction is further supported by our recent calculations in which we computed the energetics for the molecular system at various geometries. It is found that for all the potential energy surfaces with ground state  $O_2$  characteristics,  $NaO_2$  is the dominant product in the exit channel. The details of the calculations will be reported in a forthcoming paper.

## VI. References

- [1] Permanent address: Synchrotron Radiation Research Center, Hsinchu Science-based Industrial Park, Hsinchu 30077, Taiwan, ROC.
- [2] Current address: Department of Chemistry, University of Minnesota, Minneapolis, MN 55415.
- [3] Current address: Academia Sinica, Taipei, Taiwan, ROC.
- [4] E. Bulewicz, C. G. James, and T. M. Sugden, Proc. R. Soc. London **235**, 89, (A1956).
- [5] M. J. McEwan, and L. F. Phillips, Combust. Flame **9**, 420 (1965); *ibid.* **11**, 63, (1967).
- [6] C. H. Muller, K. Schofield, and M. Steinberg, J. Chem. Phys. **72**, 6620, (1980).
- [7] V. Kempter, W. Mecklenbrauck, M. Menzinger, and Ch. Schlier, Chem. Phys. Lett. **11**, 353, (1971).
- [8] H. Hou, K. T. Lu, A. G. Suits, and Y. T. Lee, Unpublished results.
- [9] A. W. Kleyn, Ph. D. Thesis, Stichting voor Fundamenteel Onderzoek der Materie, Amsterdam, The Netherlands, (1982).
- [10] A. W. Kleyn, M. M. Hubers, and J. Los, Chem. Phys. **34**, 55, (1978).
- [11] JANAF Thermochemical Tables, 3rd ed., J. Physical and Chemical Ref. Data, **14**, (1985), Supp. No.1.
- [12] D. R. Lide, Editor-in-Chief, *CRC Handbook of Chemistry and Physics*, 74th edition (1993-1994).
- [13] K. P. Huber and G. Herzberg, *Molecular Spectra and Molecular Structure, IV. Constants of Diatomic Molecules*, Van Nostrand Reinhold Company (1979).
- [14] H. Figger, W. Schrepp, and X. Zhu, J. Chem. Phys. **79**, 1320, (1983).
- [15] A. Goerke, G. Leipelt, H. Palm, C. P. Schulz, and I. V. Hertel, Z. fur Physik D **32**, 311, (1995).
- [16] Magee, J. Chem. Phys. **8**, 687, (1940).
- [17] A. W. Kleyn, in: *Alkali Halide Vapors*, edited by P. Davidovits and D. L. McFadden, Academic Press, (1979).
- [18] D. R. Herschbach, Appl. Opt. Supp. 2, 128 (1965).
- [19] R. D. Levine and R. B. Bernstein, *Molecular Reaction Dynamics and Chemical Reactivity*, Oxford University, New York (1987).
- [20] Y. T. Lee, J. D. McDonald, P. R. LeBreton, and D. R. Herschbach, Rev. Sci. Instrum. **40**, 1042, (1969).
- [21] H. F. Davis, A. G. Suits, and Y. T. Lee, J. Chem. Phys. **96**, 6710, (1992) and the references therein.

- [22] D. R. Herschbach, Disc. Faraday Soc. **33**, 149, (1962).
- [23] Y. T. Lee, in: *Atomic and Molecular Beam Methods, Vol. 1*, edited by G. Scoles, Oxford University Press, New York, (1988)
- [24] W. B. Miller, S. A. Safron, and D. R. Herschbach, J. Chem. Phys. **56**, 3581, (1972).
- [25] M. Covinsky, Ph.D. Thesis, University of California at Berkeley, (1990).
- [26] M. Steinberg and K. Schofield, J. Chem. Phys. **94**, 3901, (1991).
- [27] R. H. McFarland and J. D. Kinney, Phys. Rev. **137**, A1058, (1965).
- [28] P. S. Weiss, Ph. D Thesis, Chapter III, University of California at Berkeley, (1985).
- [29] Millard H. Alexander, J. Chem. Phys. **69**, 3502, (1978).
- [30] L. Andrews, J. Chem. Phys. **54**, 4935, (1971); R. R. Smardzewski and L. Andrews, J. Phys. Chem. **77**, 801, (1973); L. Andrews, J. T. Hwang, and C. Trindle, *ibid.* **77**, 1065, (1973).
- [31] H. Huber and G. A. Ozin, J. Mol. Spectrosc. **41**, 595, (1972).
- [32] D. M. Lindsay, D. R. Herschbach and A. L. Kwigram, Chem. Phys. Lett. **25**, 175, (1974).
- [33] P. A. G. O'Hare and A. C. Wahl, J. Chem. Phys. **56**, 4516, (1972).
- [34] W. S. Struve, J. R. Krenos, D. L. McFadden, and D. R. Herschbach, J. Chem. Phys. **62**, 404, (1975).
- [35] L. King and D. R. Herschbach, Faraday Disc. Chem. Soc. **55**, 331, (1973).
- [36] A. G. Suits, H. Hou, and Y. T. Lee, J. Phys. Chem. **94**, 5672, (1990).
- [37] K. T. Lu, H. Hou, A. G. Suits, and Y. T. Lee, unpublished results.

## VII. Figure Captions

- Fig. 1 The energy level diagram for  $\text{Na}_2 + \text{O}_2$ . Shaded regions indicate the uncertainties in the energetics. Computation is done based on changes in the bond dissociation energies  $\Delta D_0$  for each reaction. Values for  $D_0(\text{Na-O})$ ,  $D_0(\text{O-O})$  and  $D_0(\text{Na-Na})$  are from standard handbooks.[11][12][13]  $D_0(\text{Na-ONa})$  is from the results of M. Steinberg and K. Schofield[26].  $D_0(\text{Na-O}_2)$  is from the results of H. Figger and coworkers.[14] The energy of  $\text{Na}_2\text{O}_2$  complex is obtained from our *ab initio* calculation using *Gaussian 92*.[37]
- Fig. 2 Newton Diagram for  $\text{Na}_2 + \text{O}_2$  at nominal collision energy  $E_c = 8$  kcal/mol. The Circle indicates the limiting velocity of the ground state  $\text{NaO}_2$  products obtained using Equation (1).  $\Theta_{\text{CM}}$  is the  $\text{Na}_2/\text{O}_2$  center of mass angle.  $\Theta_m$  indicates the angle of  $\text{Na}/\text{O}_2$  center of mass, where we observed maximum signal for  $\text{NaO}_2$  channel.
- Fig. 3 Time-of-flight spectra measured for  $m/e = 39$  ( $\text{NaO}^+$ ) at collision energy 8 kcal/mol.  $\text{NaO}^+$  is from the electron impact fragmentation of  $\text{NaO}_2$ . Open circles are the experimental data. Solid lines indicate the best fit using  $P(E)$  and  $T(\theta)$  shown in Fig. 5.
- Fig. 4 Laboratory angular distribution of  $\text{NaO}^+$  signal at  $E_c = 8$  kcal/mol. Open circles are experimental data. Solid line is the fit using  $P(E)$  and  $T(\theta)$  shown in Fig. 5.
- Fig. 5 Product center of mass translational energy distribution  $P(E)$  and angular distribution  $T(\theta)$  that best fit the experimental data.
- Fig. 6 Newton Diagram for  $\text{Na}_2 + \text{O}_2$  at nominal collision energy  $E_c = 23$  kcal/mol. The circles indicate the limiting velocities of the ground state products.  $\Theta_{\text{CM}}$  is the  $\text{Na}_2/\text{O}_2$  center of mass angle.  $\Theta_m$  indicates the angle of  $\text{Na}/\text{O}_2$  center of mass, where we observed maximum signal for  $\text{NaO}_2$  channel.
- Fig. 7 Time-of-flight spectra measured for  $m/e = 39$  ( $\text{NaO}^+$ ) at collision energy 23 kcal/mol.  $\text{NaO}^+$  is from the both  $\text{NaO}_2$  and  $\text{NaO}$  channel. Open circles are the experimental data. Solid lines indicate the total fit. Dotted lines indicate

the contribution from the  $\text{NaO}_2 + \text{Na}$  channel and dash lines indicate the contribution from the  $\text{NaO} + \text{NaO}$  channel.

Fig. 8 Laboratory angular distribution of  $\text{NaO}^+$  signal at  $E_c = 23$  kcal/mol. Solid line indicates the total fit. The dotted line indicates the contribution from the  $\text{NaO}_2 + \text{Na}$  reaction channel, and the dash line is for the  $\text{NaO} + \text{NaO}$  channel.

Fig. 9 Translational energy distribution  $P(E)$  and angular distribution  $T(\theta)$  that best fit  $\text{NaO}_2$  channel.

Fig. 10 Translational energy distribution  $P(E)$  and angular distribution  $T(\theta)$  that best fit  $\text{NaO}$  channel.

Fig. 11  $\text{Na}^+$  time-of-flight spectra from  $\text{Na}/\text{Na}_2 + \text{O}_2$  (Left) and  $\text{Na}/\text{Na}_2 + \text{N}_2$  (Right). Open circles are the experimental data. The total fit (solid lines) is composed of four channels including elastic scattering (the fastest, dash-dot-dot), inelastic scattering (the second fastest, long dash),  $\text{NaO}_2$  channel (dash-dot) and  $\text{NaO}$  channel (short dash).

Fig. 12 Schematic drawing that illustrates the relations between the observed signal and various products.  $\sigma_i$  and  $\sigma_{iii}$  are the reaction cross sections for Reaction (i) and Reaction (iii), respectively.  $\sigma_{\text{elastic}}$  and  $\sigma_{\text{inelastic}}$  are the cross sections for the elastic scattering and the inelastic scattering of  $\text{Na} + \text{O}_2$ .  $\sigma_{\text{ion}}$ 's are the ionization cross sections by electron bombardment. The ions so formed undergo further dissociation to give observed signal.  $\xi$  is defined as the fraction of  $\text{NaO}^+$  among the total Na-containing positive ions produced by electron bombardment of  $\text{NaO}_2$ . According to the assumption that  $\text{NaO}_2$  dissociate completely upon electron bombardment, the fraction of  $\text{Na}^+$  from  $\text{NaO}_2$  is  $(1-\xi)$ .  $\eta$  is defined as the fraction of  $\text{Na}^+$  among the total Na-containing positive ions from the ionization of  $\text{NaO}$ .

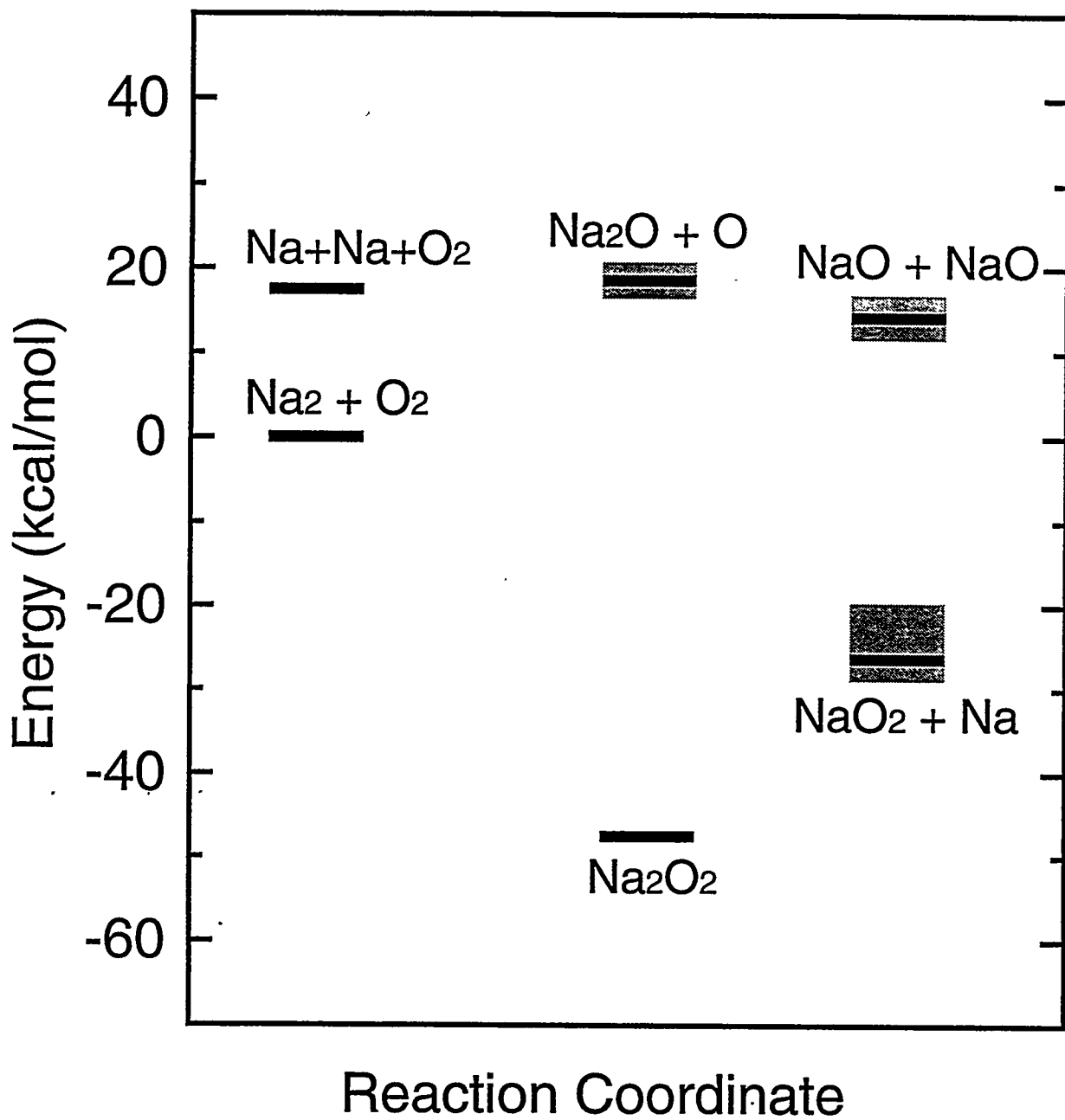


Figure 1.

$$E_c = 8 \text{ kcal/mol}$$

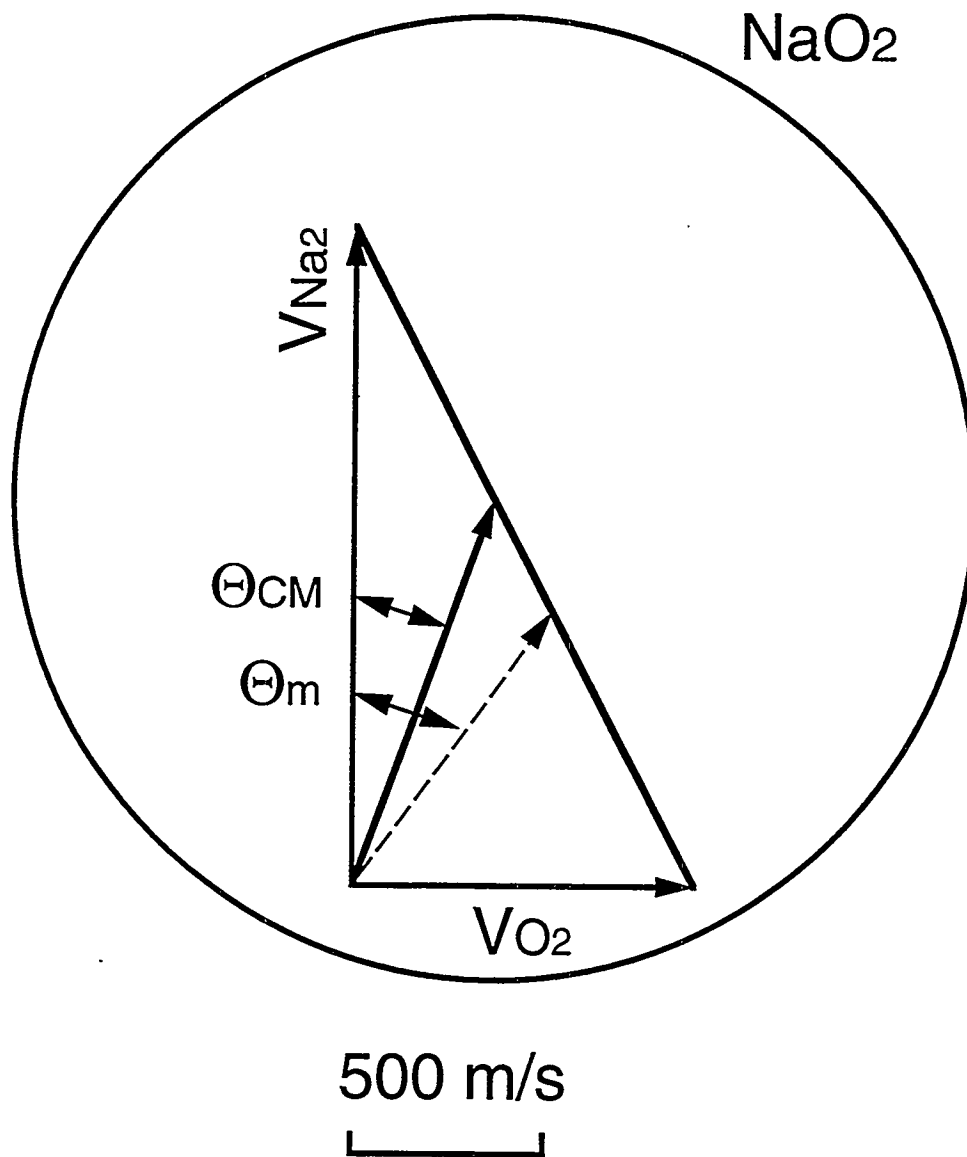


Figure 2.

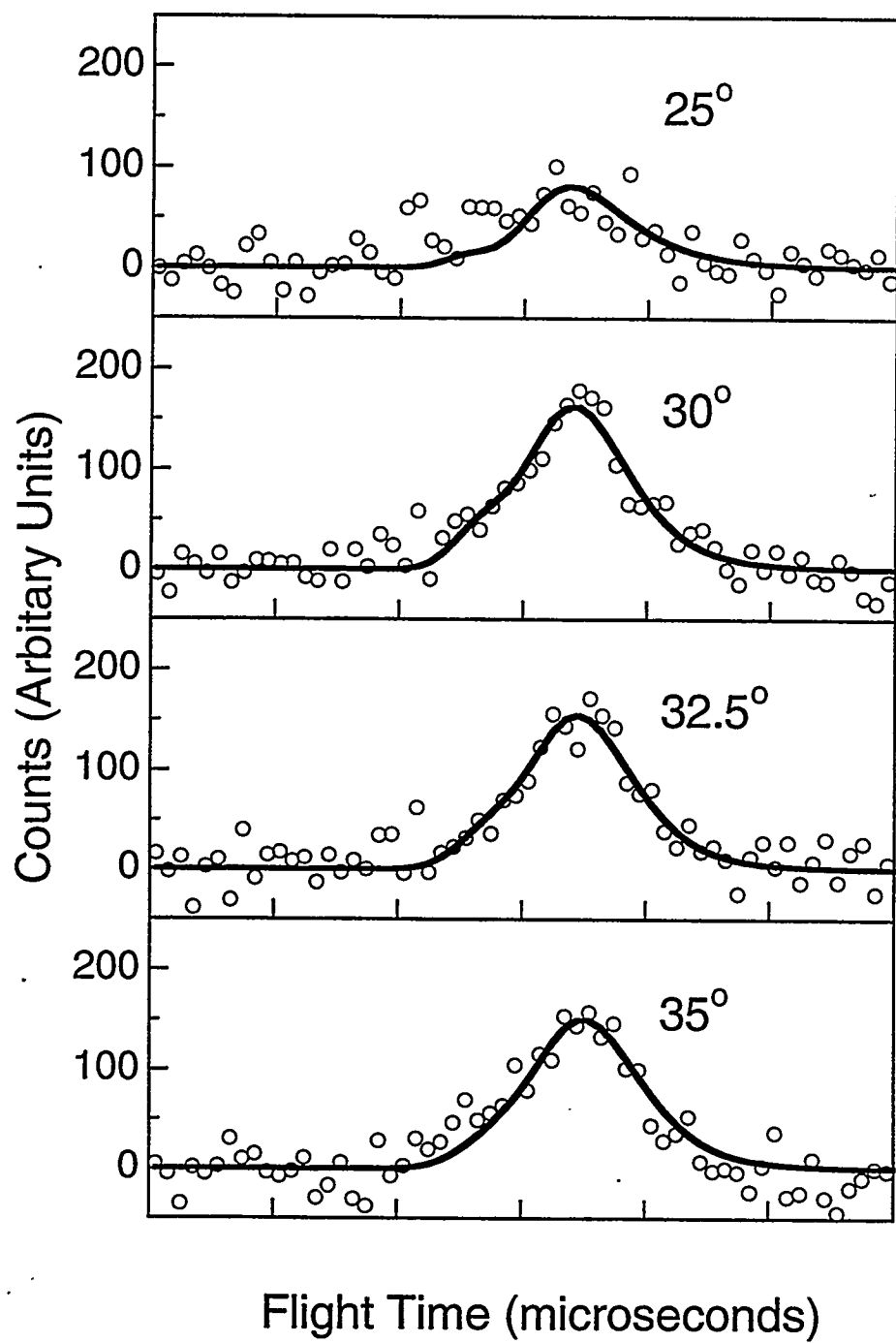


Figure 3.

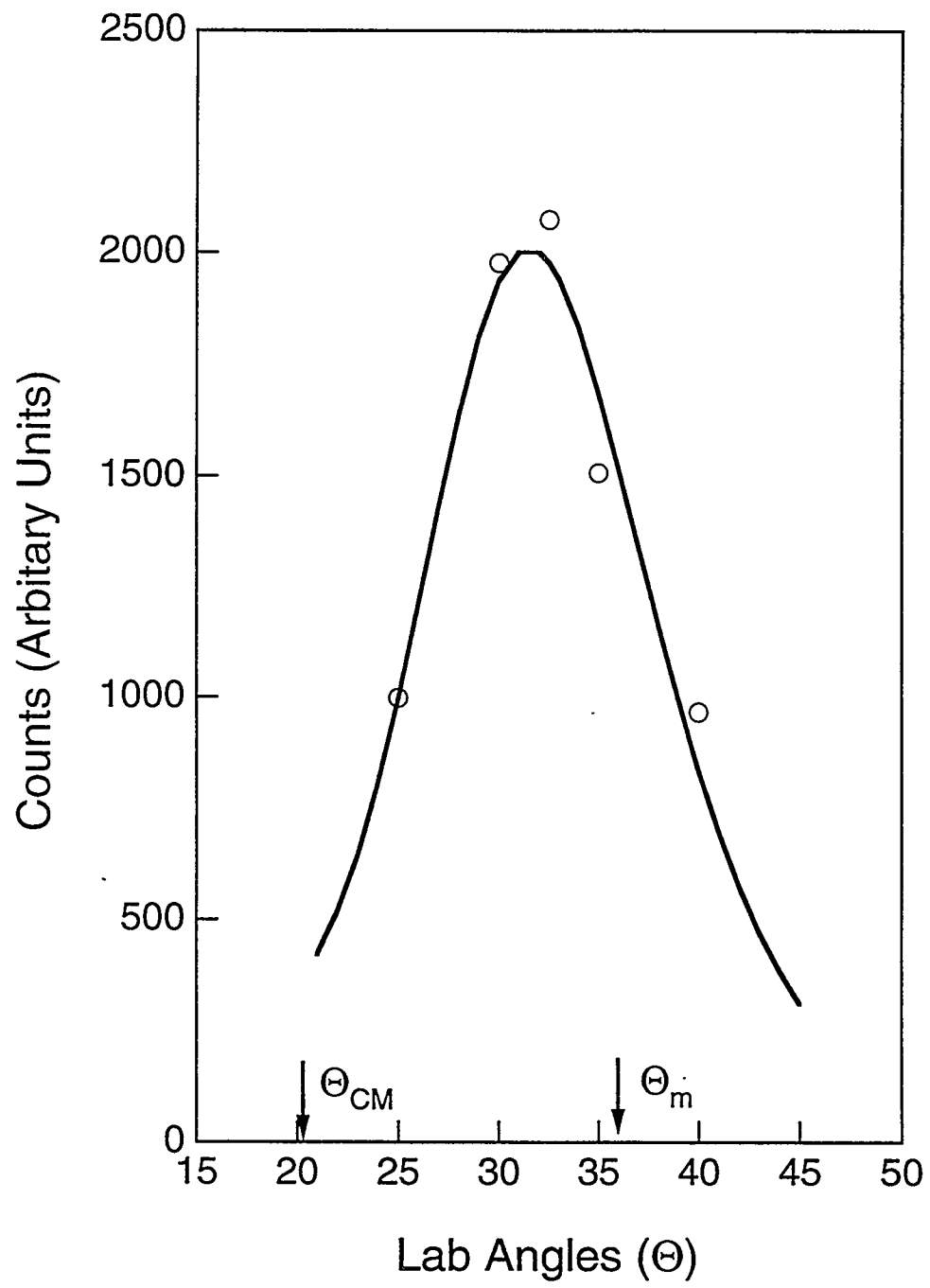


Figure 4.

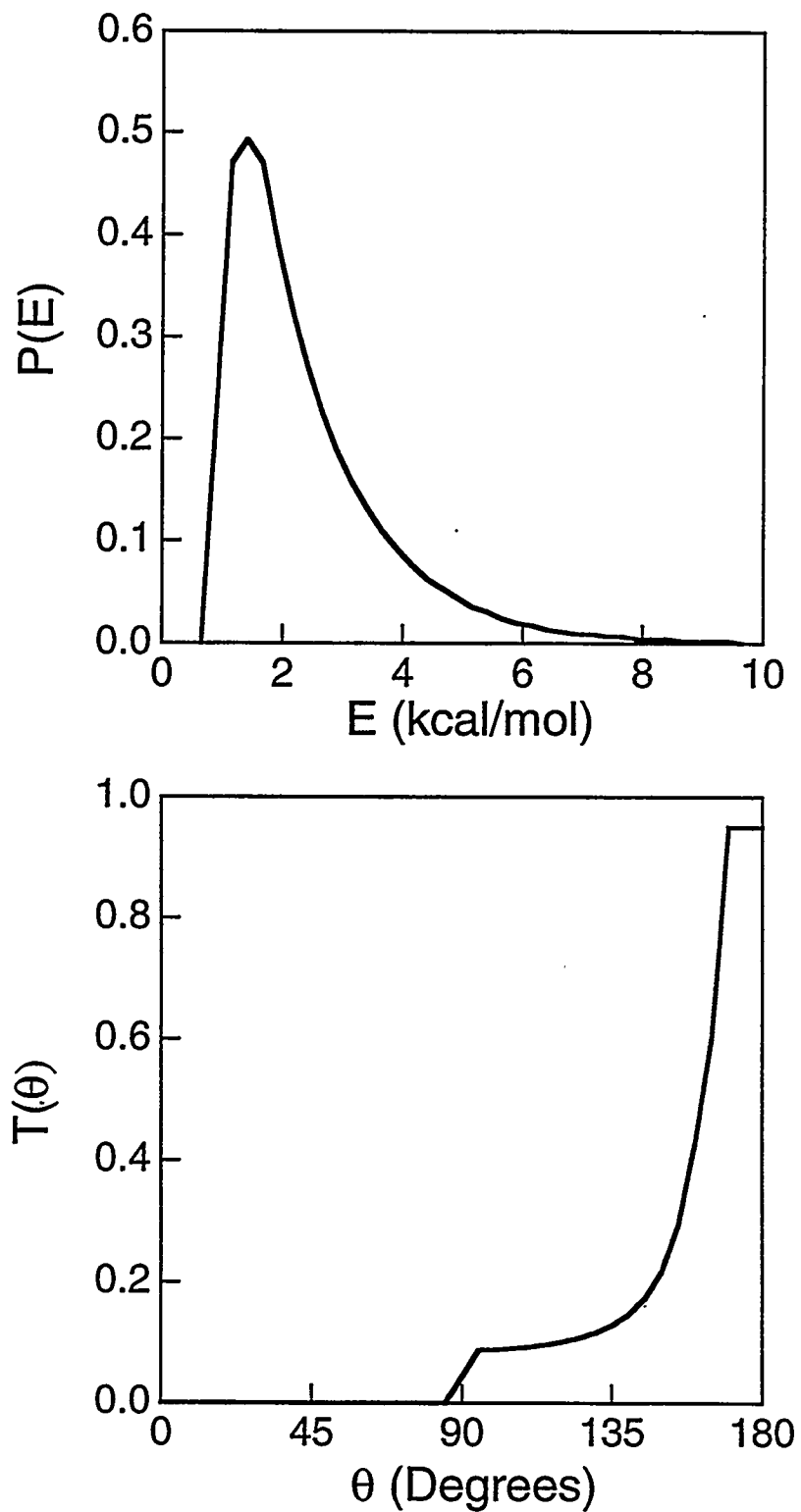


Figure 5

$$E_c = 23 \text{ kcal/mol}$$

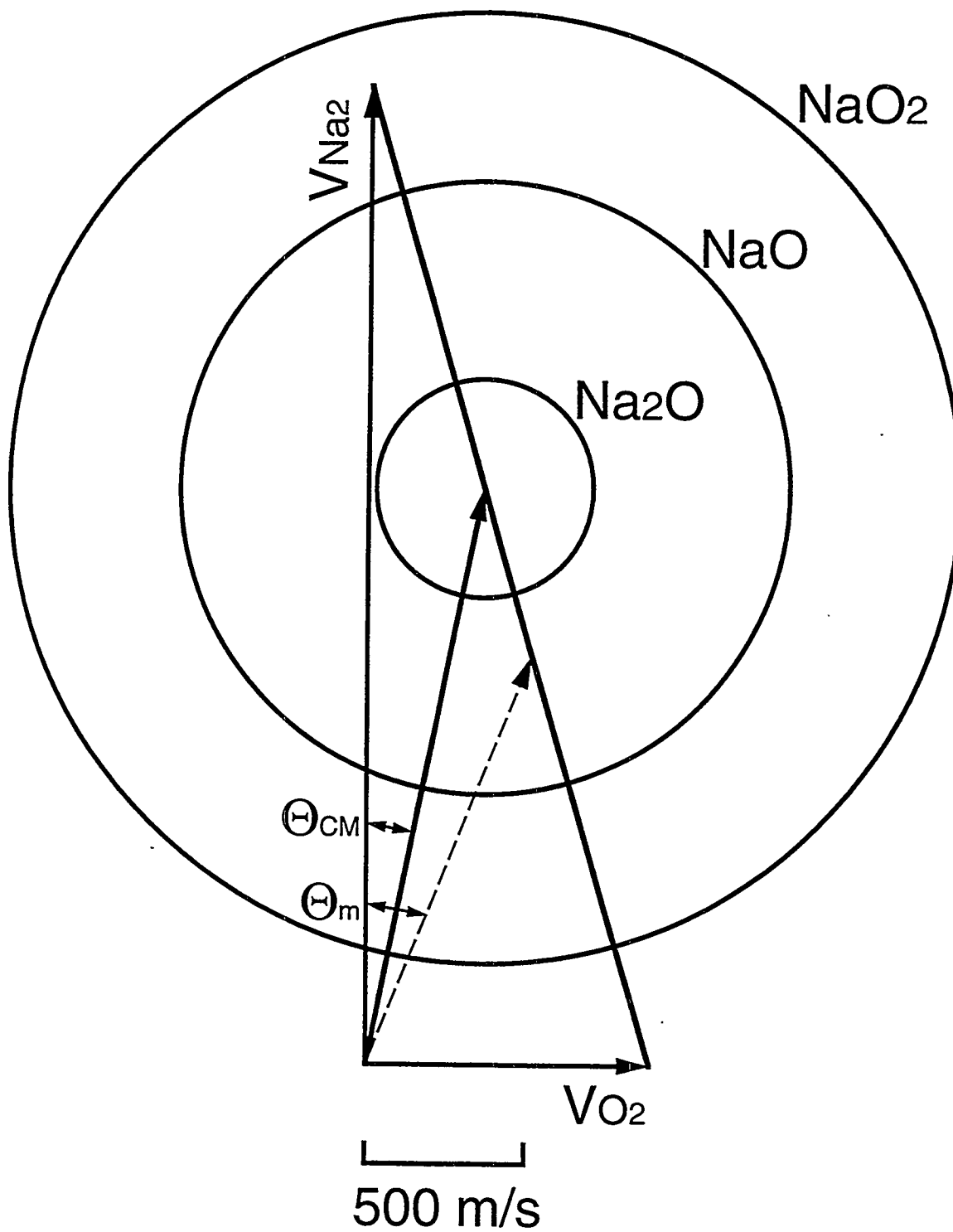


Figure 6.

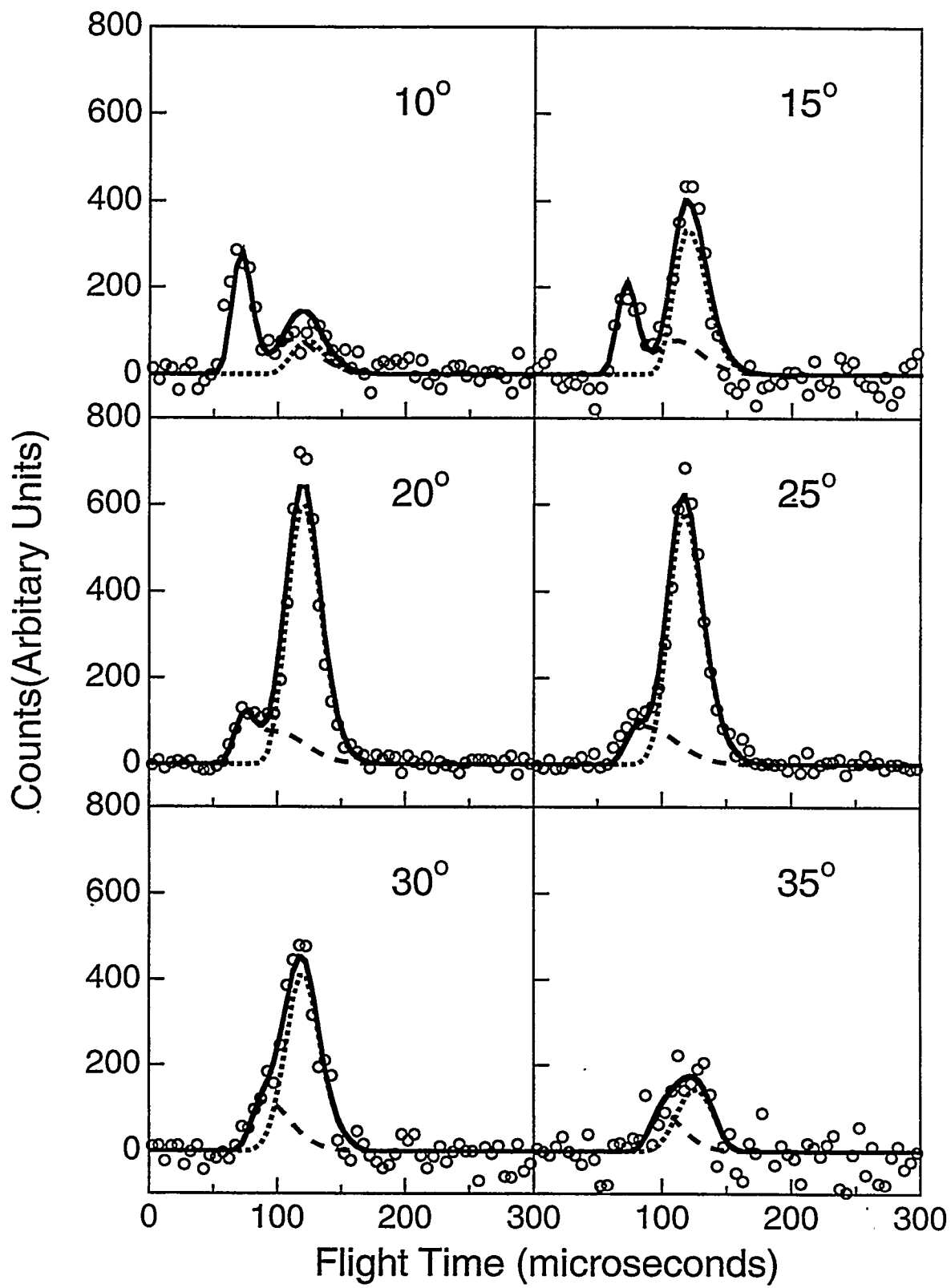


Figure 7.

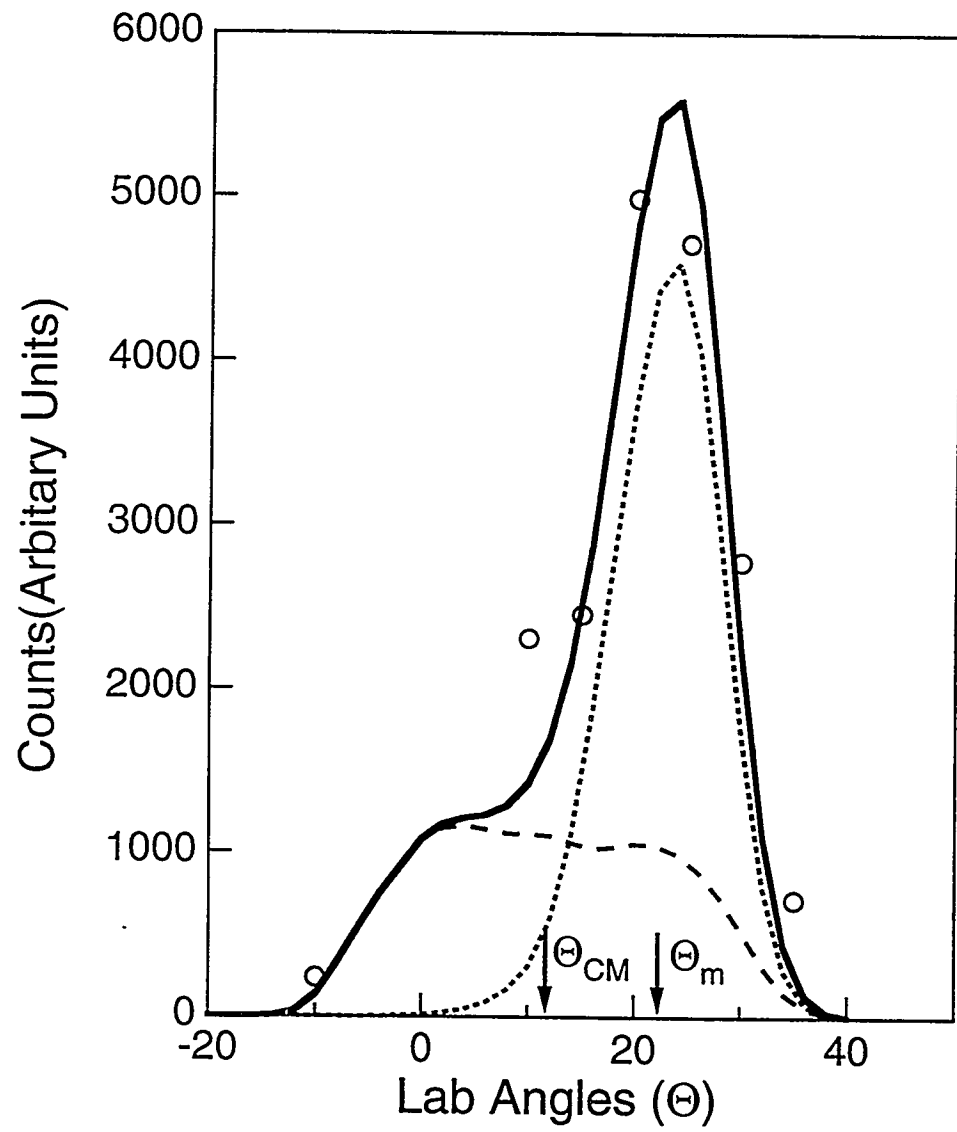


Figure 8.

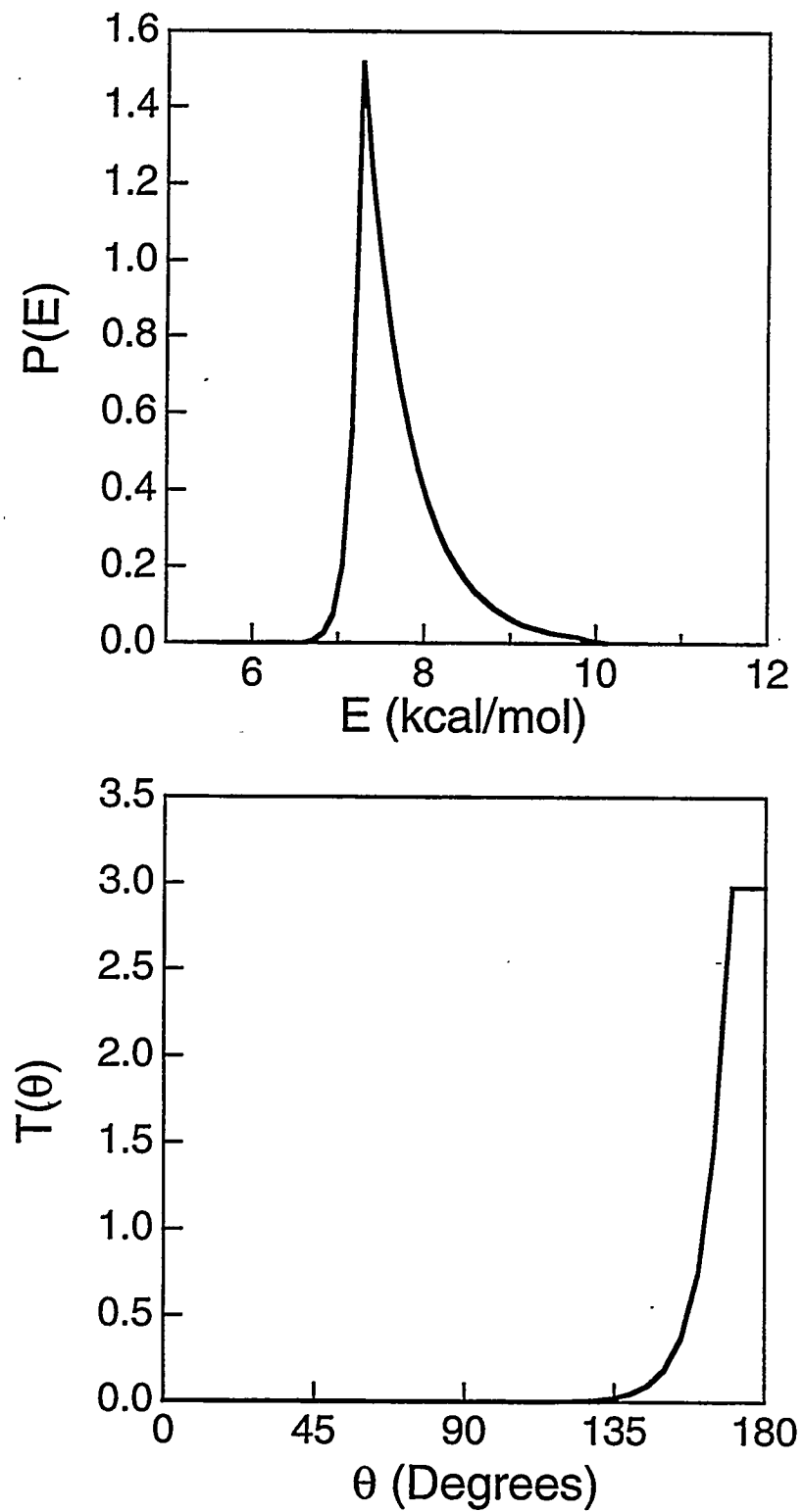


Figure 9.

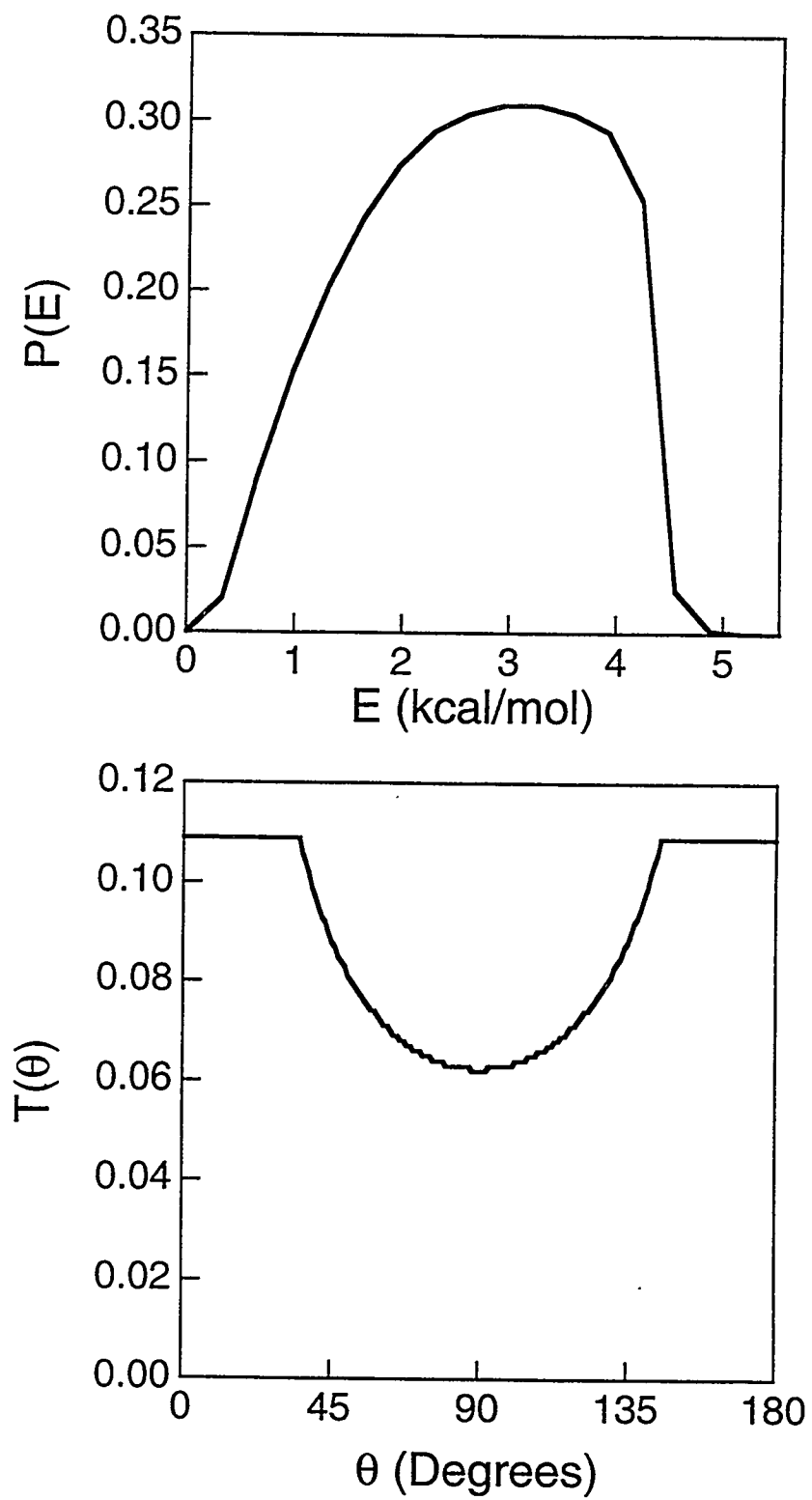


Figure 10.

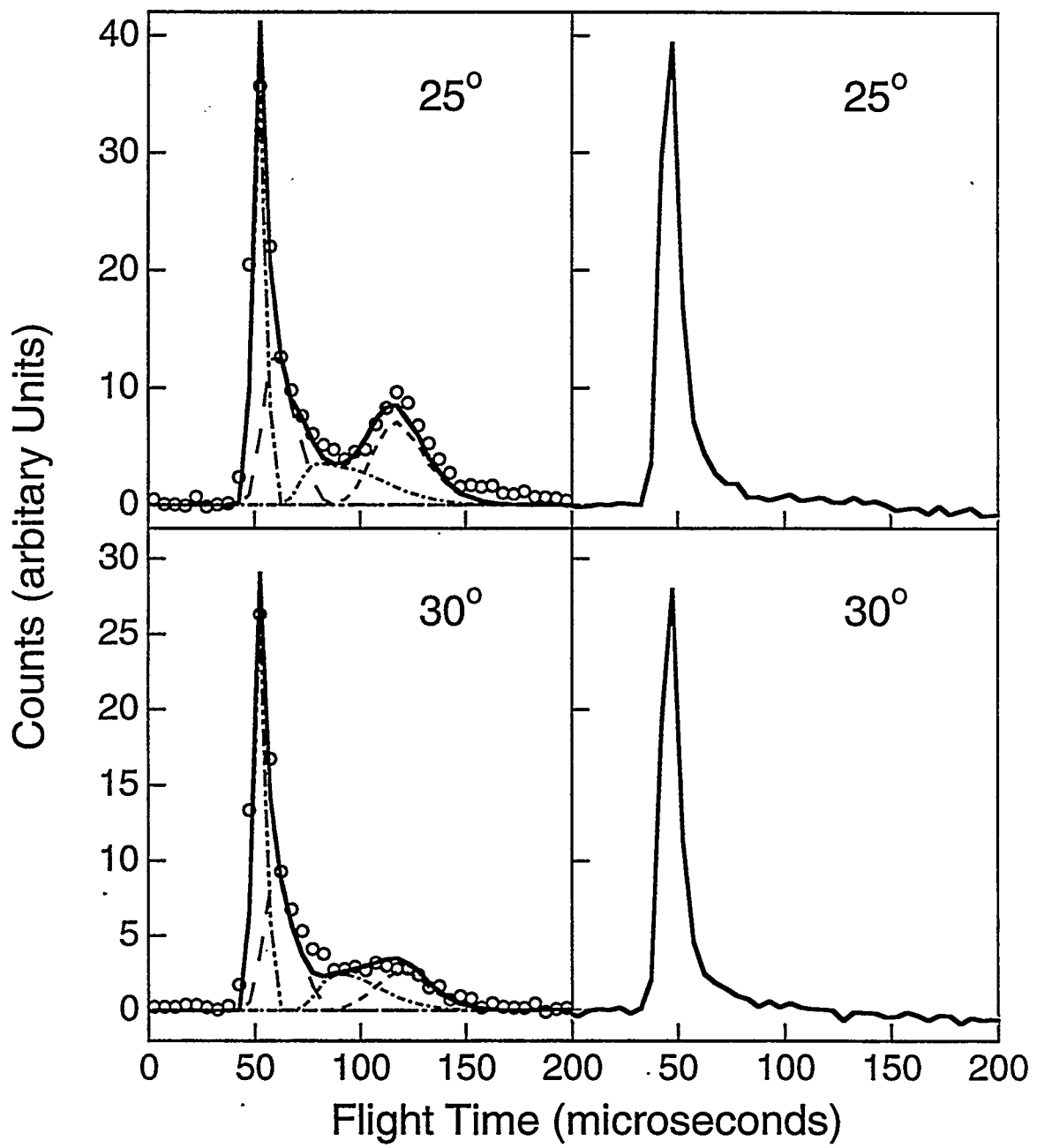


Figure 11.

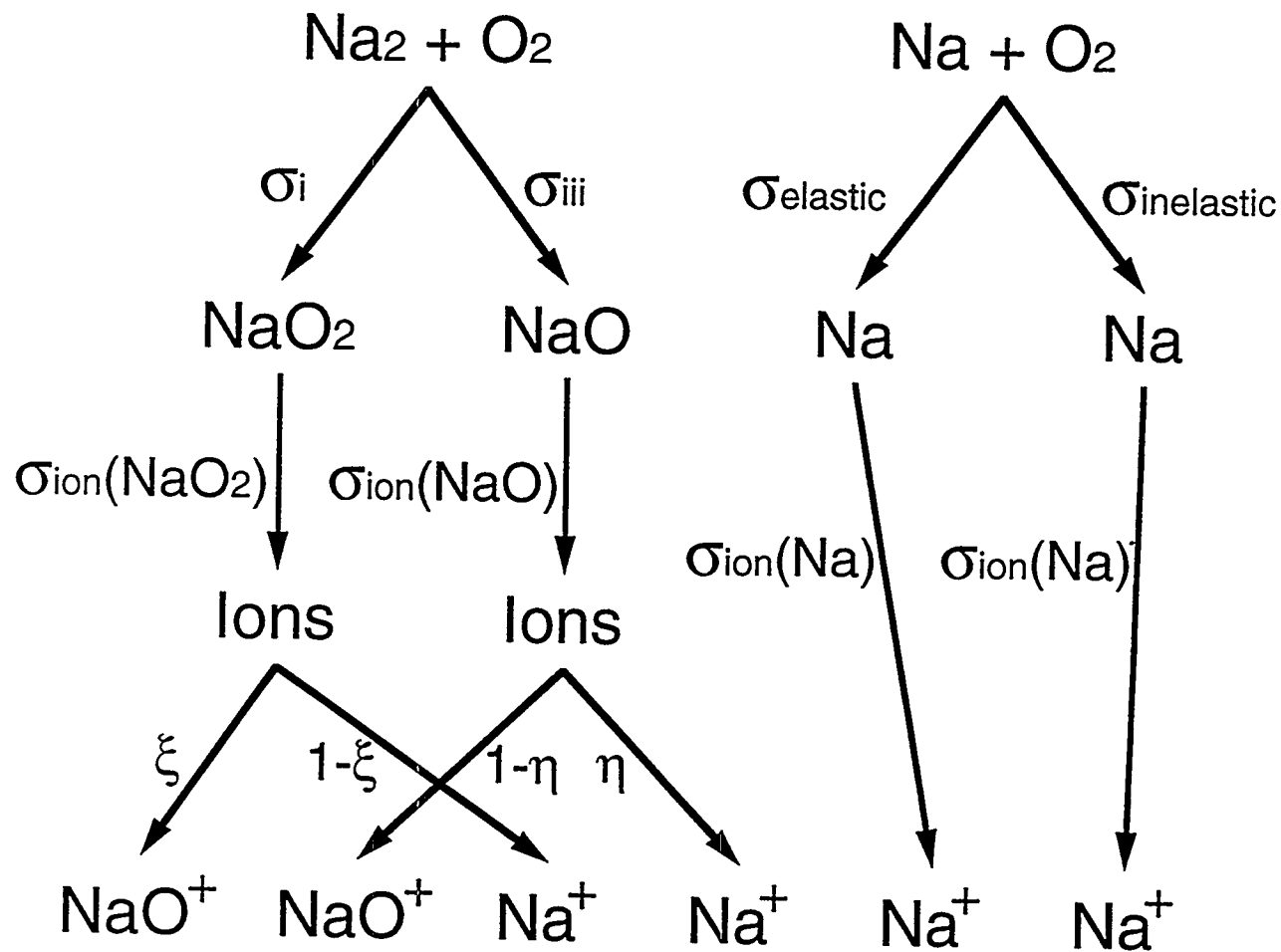


Figure 12